nArgBP2 regulates excitatory synapse formation by controlling dendritic spine morphology

Sang-Eun Lee[a,b], Yoonju Kim[a,b,c], Jeong-Kyu Han[a,d], Hoyong Park[e], Unghwi Lee[a,b], Myeongsu Na[a,b], Soomin Jeong[a,b], ChiHye Chung[e], Gianluca Cestra[f,g,1], and Sunghoe Chang[a,b,d,1]

[a]Department of Physiology and Biomedical Sciences, Seoul National University College of Medicine, Seoul 01030, South Korea; [b]Biomembrane Plasticity Research Center, Seoul National University College of Medicine, Seoul 01030, South Korea; [c]KM Convergence Research Division, Korea Institute of Oriental Medicine, Daejeon 34054, South Korea; [d]Interdisciplinary Program in Neuroscience, Seoul National University College of Medicine, Seoul 01030, South Korea; [e]Department of Biological Sciences, Konkuk University, Seoul 05029, South Korea; [f]Istituto di Biologia e Patologia Molecolari, Consiglio Nazionale delle Ricerche, 00185 Rome, Italy; and [g]Department of Biology and Biotechnology, University of Rome "Sapienza", 00185 Rome, Italy

Edited by Solomon H. Snyder, Johns Hopkins University School of Medicine, Baltimore, MD, and approved April 28, 2016 (received for review January 18, 2016)

Neural Abelson-related gene-binding protein 2 (nArgBP2) was originally identified as a protein that directly interacts with synapse-associated protein 90/postsynaptic density protein 95-associated protein 3 (SAPAP3), a postsynaptic scaffolding protein critical for the assembly of glutamatergic synapses. Although genetic deletion of nArgBP2 in mice leads to manic/bipolar-like behaviors resembling many aspects of symptoms in patients with bipolar disorder, the actual function of nArgBP2 at the synapse is completely unknown. Here, we found that the knockdown (KD) of nArgBP2 by specific small hairpin RNAs (shRNAs) resulted in a dramatic change in dendritic spine morphology. Reintroducing shRNA-resistant nArgBP2 reversed these defects. In particular, nArgBP2 KD impaired spine-synapse formation such that excitatory synapses terminated mostly at dendritic shafts instead of spine heads in spiny neurons, although inhibitory synapse formation was not affected. nArgBP2 KD further caused a marked increase of actin cytoskeleton dynamics in spines, which was associated with increased Wiskott–Aldrich syndrome protein-family verprolin homologous protein 1 (WAVE1)/p21-activated kinase (PAK) phosphorylation and reduced activity of cofilin. These effects of nArgBP2 KD in spines were rescued by inhibiting PAK or activating cofilin combined with sequestration of WAVE. Together, our results suggest that nArgBP2 functions to regulate spine morphogenesis and subsequent spine-synapse formation at glutamatergic synapses. They also raise the possibility that the aberrant regulation of synaptic actin filaments caused by reduced nArgBP2 expression may contribute to the manifestation of the synaptic dysfunction observed in manic/bipolar disorder.

nArgBP2 | dendritic spines | excitatory synapse | actin | bipolar disorder

The postsynaptic enriched adaptor protein neural Abelson-related gene-binding protein 2 (nArgBP2), a neural-specific splice variant of the ubiquitous ArgBP2, was originally identified as a binding partner of synapse-associated protein 90/postsynaptic density protein 95-associated protein 3 (SAPAP3) (1). It belongs to a family of adaptor proteins that are involved in the regulation of cell adhesion, actin cytoskeleton organization, and growth factor receptor signaling (2). This protein family is characterized by a sorbin homology (SoHo) domain in the NH_2-terminal region and three Src homology 3 (SH3) domains in the COOH-terminal region (3). Although the SoHo domain remains poorly characterized, the SH3 domains bind signaling protein kinases, the ubiquitin ligase, and protein involved in the regulation of focal adhesions and adhering junctions (1, 4–6). The NH_2-terminal region of nArgBP2, which contains the SoHo domain, interacts with spectrin, whereas the COOH-terminal SH3 domains bind dynamin, synaptojanin, Wiskott–Aldrich syndrome protein-family verprolin homologous protein (WAVE) isoforms, and WAVE regulatory proteins (3), all of which participate in the regulation of the actin cytoskeleton. We also found that the down-regulation of both ArgBP2 and nArgBP2 expression in astrocytes redistributes focal adhesion proteins and increases peripheral actin ruffles (3), suggesting that nArgBP2 controls the balance between adhesion and motility by coordinating actin cytoskeleton dynamics.

WAVE and Rac1 are key players in the regulation of actin dynamics. WAVE activates the actin-related protein (Arp2/3) complex (7), and its phosphorylation by cyclin-dependent kinase 5 is known to regulate dendritic spine morphology (8). Rac1 also regulates dendrite initiation, elongation, and the complexity of branching, as well as spine formation (9, 10). The major downstream effector of Rac1 is p21-activated kinase (PAK), which controls LIM-domain containing protein kinase (LIMK), which, in turn, facilitates actin filament stabilization through the phosphorylation and inactivation of the actin depolymerizing factor cofilin (11–14). Aberrant WAVE/Rac1/PAK signaling leads to defects in neuronal connectivity and synaptic plasticity (15, 16). Importantly, genetic analyses have revealed that mutations in genes regulating the actin filament network at synapses are associated with intellectual disability (17), autism (18), and schizophrenia (19), indicating dysregulation of actin cytoskeleton as one of the common pathophysiological mechanisms for these disorders.

nArgBP2 mRNA is highly expressed in the isocortex, hippocampal formation, cortical subplate, striatum, thalamus, and hypothalamus (20), the majority of which are regions of the brain associated with bipolar disorder (BD) (21). Furthermore, genetic

Significance

Recent studies have implicated postsynaptic scaffolding protein synapse-associated protein 90/postsynaptic density protein 95-associated protein 3 (SAPAP3) or Shank3 in mood disorders such as bipolar disorder, autism, and obsessive-compulsive disorders. Neural Abelson-related gene-binding protein 2 (nArgBP2) is a binding partner of both SAPAP3 and Shank3, and its genetic deletion in mice leads to manic/bipolar-like behavior resembling symptoms of bipolar disorder. Remarkably, nothing is known about the synaptic function of nArgBP2 or its connection with the synaptic alterations associated with bipolar disorder. Here, we provide compelling evidence that nArgBP2 regulates spine morphogenesis and that its ablation causes a robust and selective inhibition of excitatory synapse formation by controlling actin dynamics. Our results revealed the underlying mechanism for the synaptic dysfunction caused by nArgBP2 down-regulation that may be associated with human bipolar disorder.

Author contributions: G.C. and S.C. designed research; S.-E.L., Y.K., J.-K.H., H.P., U.L., M.N., S.J., and G.C. performed research; S.-E.L., Y.K., J.-K.H., H.P., U.L., M.N., S.J., C.C., G.C., and S.C. analyzed data; and S.-E.L., C.C., G.C., and S.C. wrote the paper.

The authors declare no conflict of interest.

This article is a PNAS Direct Submission.

[1]To whom correspondence may be addressed. Email: sunghoe@snu.ac.kr or gianluca.cestra@uniroma1.it.

This article contains supporting information online at www.pnas.org/lookup/suppl/doi:10.1073/pnas.1600944113/-/DCSupplemental.

NEUROSCIENCE

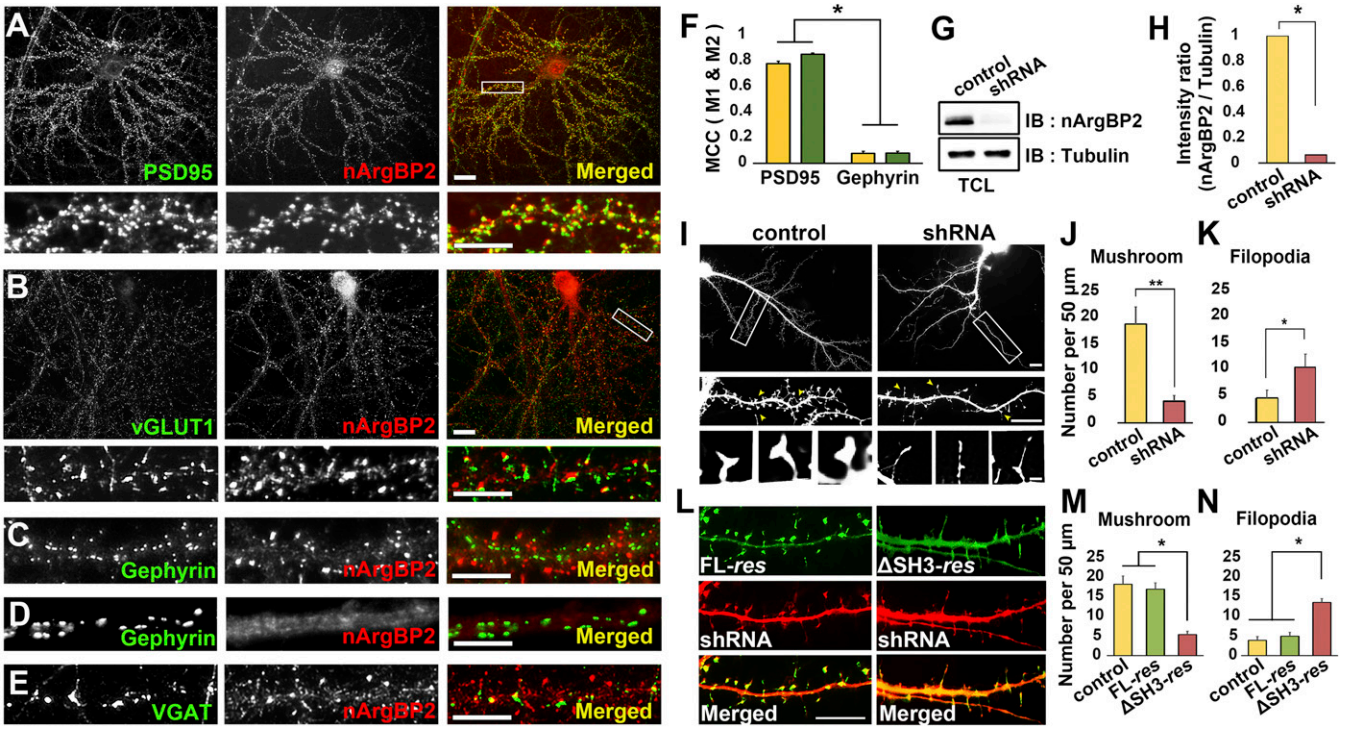

Fig. 1. nArgBP2 primarily localizes to excitatory synapses in spiny neurons, and KD of nArgBP2 decreases mushroom-shaped spines and increases filopodia-like protrusions. nArgBP2 clusters colocalized with PSD95 (*A*) and were also juxtaposed with vGLUT1 puncta in pyramidal spiny neurons (*B*). (*Lower*) Images are enlarged views of the boxed regions. nArgBP2 clusters did not colocalize with gephyrin in spiny neurons (*C*) and were almost absent in aspiny neurons (*D*). (*E*) nArgBP2 rarely colocalized with vGAT in spiny neurons. (Scale bars: *A* and *B*, *Upper*, 20 μm; *A* and *B*, *Lower* and *C*–*E*, 10 μm.) (*F*) Manders' colocalization coefficients (MCCs) of nArgBP2 clusters with PSD95 or gephyrin signals. M1 (yellow bars) indicates the fraction of nArgBP2 overlapping PSD95 or gephyrin, and M2 (green bars) indicates the fraction of PSD95 or gephyrin overlapping nArgBP2 (M1: 0.78 ± 0.02 for PSD95, 0.08 ± 0.02 for gephyrin; M2: 0.85 ± 0.01 for PSD95, 0.08 ± 0.01 for gephyrin). (*G* and *H*) Cortical neurons at DIV6 were infected with adenoassociated virus (AAV)-shRNA-nArgBP2, and the KD efficiency was confirmed by Western blotting with anti-nArgBP2 antibody at DIV21. (*I*) Representative spine morphologies from dendrites of neurons expressing scrambled (control) or shRNA-nArgBP2. Hippocampal neurons were transfected at DIV9 and fixed at DIV16. (*Middle*) Enlarged images of parts enclosed with rectangles. (*Lower*) Three representative examples of mushroom spines from control neurons and filopodia-shaped protrusions from nArgBP2 KD. (Scale bars: *Upper* and *Middle*, 20 μm; *Lower*, 2 μm.) The numbers of mushroom-shaped spines (*J*) and filopodia (*K*) from control and shRNA-transfected neurons are shown. $*P < 0.05$; $**P < 0.01$ by Student's *t* test ($n = 54$ neurons from six independent cultures). (*L*) Representative images of spine morphologies from dendrites of neurons coexpressing the shRNA with GFP full-length nArgBP2 (FL)–resistant or GFP-ΔSH3-nArgBP2 (ΔSH3)–resistant constructs. *res*, a silent mutation that is resistant to shRNA. (Scale bar: 20 μm.) The numbers of mushroom-shaped spines (*M*) and filopodia (*N*) are shown ($n = 36$ neurons from five independent cultures).

deletion of nArgBP2 in mice leads to manic/bipolar-like behavior resembling many symptoms of BD (22, 23). A recent study also showed that genetic deletion of SAPAP3, a binding partner of nArgBP2, causes anxiety-like behaviors in mice, thus implicating it in the pathogenesis of obsessive-compulsive behaviors (24). Another recent study has shown overexpressed SH3 and multiple ankyrin repeat domains 3 (Shank3) causes manic-like behaviors (25), whereas loss of Shank3 is linked to autism spectrum disorders (26, 27). Interestingly, Shank3 binds to SAPAP, which interacts directly with nArgBP2, again positioning nArgBP2 as a hub in the etiology of various mood disorders. Despite the high possibility that nArgBP2 could be involved in the etiology of such mood disorders, remarkably, nothing is known about the role of nArgBP2 at synapses or its connection with the synaptic dysfunctions associated with these neurological disorders.

In the current study, we found that knocking down nArgBP2 causes a dramatic change in spine morphology and a robust inhibition of excitatory spine-synapse formation. nArgBP2 down-regulation increases actin dynamics through the activation of the Rac1/WAVE/PAK pathway, which in turn decreases cofilin activity. Thus, we provide evidence that nArgBP2 regulates spine morphogenesis and glutamatergic spine-synapse formation by controlling actin dynamics. Because recent reports have shown that genetic deletion of nArgBP2 in mice leads to manic/bipolar-like behavior, our results revealed the underlying mechanism for the synaptic dysfunction caused by nArgBP2 down-regulation that may be associated with analogous human neurological disorders.

Results

In cultured hippocampal neurons, nArgBP2 signals were primarily detected in punctate clusters in dendrites that colocalized with the excitatory postsynaptic scaffolding protein PSD95 (Fig. 1 *A* and *F*). Dendritic clusters of nArgBP2 were also juxtaposed with the vesicular glutamate transporter 1 (vGLUT1; an excitatory presynaptic protein) puncta in spiny neurons (Fig. 1*B*). In contrast, nArgBP2 rarely overlapped with the inhibitory postsynaptic scaffolding protein gephyrin in spiny neurons (Fig. 1 *C* and *F*) and was almost absent in aspiny gephyrin-positive neurons (Fig. 1*D* and Fig. S1). Consistently, nArgBP2 clusters were hardly juxtaposed with the vesicular GABA transporter (vGAT; an inhibitory presynaptic protein) (Fig. 1*E* and Fig. S1). We found that nArgBP2 clusters were mainly detected in neurons negative for the GABA synthetic enzyme glutamic acid decarboxylase GAD67, whereas only nuclear and diffuse signals were observed in GAD67-positive GABAergic neurons (Fig. S1*A*). Thus, we conclude that nArgBP2 primarily localizes to excitatory synapses in spiny pyramidal neurons.

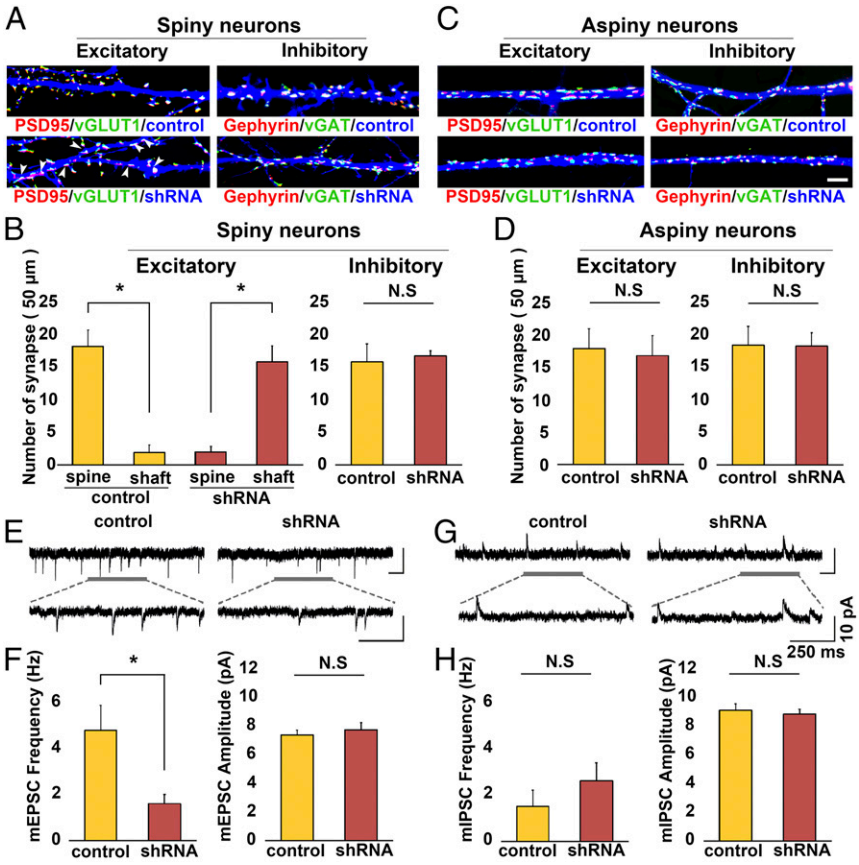

Fig. 2. nArgBP2 KD impairs excitatory spine-synapse formation, although it does not affect inhibitory synapses. (*A* and *B*) Immunocytochemistry of dendrites from scrambled (control) and nArgBP2 KD (shRNA) spiny neurons (DIV21) colabeled with antibodies against vGLUT1 and PSD95 or vGAT and gephyrin to visualize pre- and postsynaptic elements of excitatory or inhibitory synapses, respectively. Arrowheads point to PSD95 clusters that form at dendritic shafts instead of dendritic spines. (*C* and *D*) Analogous experiments to reveal excitatory and inhibitory synaptic contacts in aspiny neurons. To generate a more contrasted picture, we have pseudocolored the gephyrin signal to red and the DsRed signal by the shRNA vector to blue. The number of excitatory synaptic contacts on dendritic spines in spiny neurons (vGLUT1 and PSD95 puncta) was dramatically reduced in KD neurons, although the number of inhibitory synaptic contacts on the dendritic shaft (vGAT and gephyrin puncta) was not changed. Neither excitatory nor inhibitory contacts in aspiny neurons were altered. All data are mean ± SEM. $*P < 0.01$ ($n = 52$ neurons from five independent cultures). N.S., not significant. (Scale bar: *A* and *C*, 5 µm.) (*E* and *F*) nArgBP2 KD reduced the frequency, but not the amplitude, of mEPSCs. Neurons were transfected at DIV9 and analyzed at DIV16. Sample traces of mEPSCs are shown in *E*. $*P < 0.05$ by Student's *t* test [$n = 9$ for control (scrambled) and for KD]. (*G* and *H*) nArgBP2 KD had no effect on the frequency or amplitude of miniature inhibitory postsynaptic currents (mIPSCs) [$n = 7$ for control and 8 for KD (Student's *t* test)]. Error bars indicate mean ± SEM.

To assess the physiological effects of nArgBP2 on spine formation, we generated small hairpin RNA (shRNA) targeting all isoforms of nArgBP2. Suppression of nArgBP2 expression by shRNA was confirmed by Western blot analyses of cultured cortical neurons and GFP-nArgBP2–transfected HEK293T cells (Fig. 1 *G* and *H* and Fig. S2). To investigate the effect of nArgBP2 knockdown (KD) on dendritic spine formation, neurons were transfected at 9 d in vitro (DIV9) with shRNA or scrambled shRNA, and were fixed at DIV16. We found that the density of total dendritic protrusions was decreased in KD, but the most striking effect was on dendritic spine morphology. nArgBP2 KD resulted in a dramatic decrease in the proportion of mushroom-shaped spines (18.83 ± 3.20 for control, 4.16 ± 1.11 for KD; Fig. 1 *I* and *J*) and a concomitant increase of long, thin, filopodia-like protrusions (Fig. 1 *I* and *K*). When a GFP full-length nArgBP2 that is resistant to shRNA (GFP-nArgBP2-*res*) was introduced into KD neurons, the defect on dendritic spine morphology was fully rescued, ruling out any off-target effect of shRNA expression (Fig. 1 *L*–*N*). The SH3 domain-deletion mutant (GFP-ΔSH3-nArgBP2-*res*), however, failed to rescue the KD phenotype, indicating that the SH3-mediated interactions are required (Fig. 1 *L* and *M*).

Dendritic spines are actin-rich architectures that receive presynaptic inputs in most excitatory synapses of the central nervous system (28). To monitor excitatory/inhibitory synaptogenesis in vitro, neurons were labeled with antibodies against presynaptic vGLUT1 and postsynaptic PSD95 or presynaptic vGAT and postsynaptic gephyrin to distinguish between putative excitatory and inhibitory synapses, respectively (Fig. 2 *A*–*D*). Presynaptic development was similar in both neurons as assayed by the quantification of vGLUT1- or vGAT-positive puncta (puncta per 50 µm of dendrite; vGLUT1: 19.04 ± 1.13 for control, 17.31 ± 1.81 for KD; vGAT: 17.49 ± 1.14 for control, 17.80 ± 1.72 for KD), demonstrating that nArgBP2 KD did not interfere with the establishment of presynaptic contacts. Intriguingly, excitatory contacts between vGLUT1 and PSD95 in KD predominantly formed at dendritic shafts instead of on spine heads in spiny neurons (Fig. 2 *A* and *B*). The number of synapse on spines was decreased dramatically with concomitant increase of synapse on shafts (18.20 ± 2.50 on spines, 1.91 ± 1.08 on shaft for control and 1.899 ± 0.83 on spines, 15.81 ± 2.5 on shaft for KD; Fig. 2*B*). The location of vGAT-gephyrin–positive inhibitory contacts on dendritic shafts appeared unchanged (Fig. 2 *A* and *B*). In contrast, excitatory and inhibitory synapses in aspiny neurons were not altered by KD (Fig. 2 *C* and *D*). These data indicate that nArgBP2 KD causes a specific reduction of spine-bearing synapses, which is also consistent with the decrease in "matured" mushroom-shaped spines in nArgBP2 KD neurons.

We next evaluated the functional consequence of nArgBP2 KD on synaptic transmission. nArgBP2 KD significantly reduced the mean frequency of miniature excitatory postsynaptic currents (mEPSCs), whereas the amplitude of the mEPSCs was unaffected (Fig. 2 *E* and *F*). nArgBP2 KD had no effect on miniature inhibitory postsynaptic currents in both frequency and amplitude (Fig. 2 *G* and *H*), supporting its selective role in controlling spine-bearing excitatory synapses. We further showed that GFP-nArgBP2-*res*, but not GFP-ΔSH3 nArgBP2-*res*, rescued the defects in mEPSC frequency by KD (Fig. S2).

To address the molecular mechanisms linking loss of nArgBP2 to aberrant spine morphology, we studied actin cytoskeleton modifications (29–31). nArgBP2 interacts with WAVE and proteins of the WAVE regulatory complex like PIR121 and Nap1 (3). Thus, we followed the state of activation of WAVE in nArgBP2 KD neurons and found increased levels of phospho-WAVE1 (Fig. 3*A*), the active form of the protein.

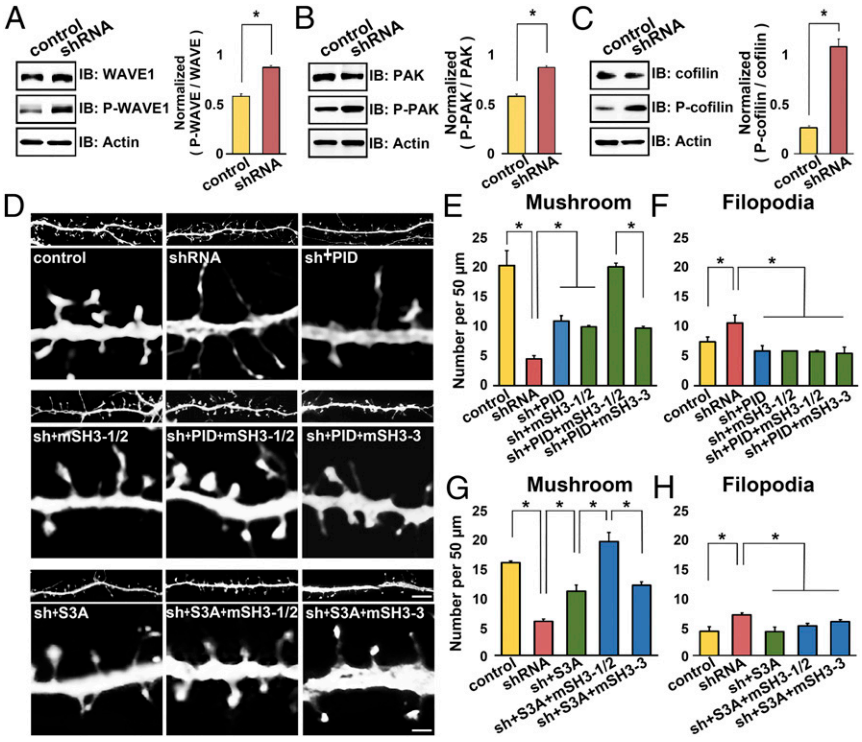

Fig. 3. nArgBP2 KD increases WAVE1/PAK/cofilin phosphorylation, and counteracting this cascade rescues nArgBP2 KD effects on spines. Cortical neurons infected with AAV-scrambled or shRNA-nArgBP2 at DIV6, lysed at DIV21, and immunoblotted with anti-WAVE1 and phospho-WAVE1 antibody (*A*), PAK and phospho-PAK antibody (*B*), and anticofilin and phosphocofilin antibody (*C*) are shown. IB, immunoblot. (*D*) Representative images of spine from dendrites of neurons expressing each set of constructs. Hippocampal neurons were transfected at DIV9 and fixed at DIV16. Control, scrambled; shRNA (sh), shRNA-nArgBP2; S3A, phosphodeficient mutant of cofilin; mSH3-1/2, first and second SH3 domains of nArgBP2 targeted to mitochondria; mSH3-3, third SH3 domain of nArgBP2 targeted mitochondria. (*Lower*) Enlarged images of the insets enclosed with rectangles. (Scale bars: *Upper*, 10 μm; *Lower*, 2 μm.) The numbers of mushroom-shaped spines (*E* and *G*) and filopodia (*F* and *H*) from each experimental group are shown. $*P < 0.05$ by ANOVA, followed by Tukey's honest significant difference (HSD) post hoc test [$n = 45$ neurons from seven independent cultures (*E* and *F*) and $n = 39$ neurons from four independent cultures (*G* and *H*)].

WAVE is activated by Rac1, which also promotes phosphorylation of cofilin via PAK-LIMK cascade (12, 32). Because the role of PAK and cofilin on spine morphogenesis is well established (15, 33–35), we hypothesized that loss of nArgBP2 may enhance Rac1 activity, leading to activation of PAK and subsequent inactivation of cofilin, which may ultimately cause the loss of mature mushroom-type spines and an overabundance of immature filopodia-like protrusions. Indeed, we also observed an up-regulation of phosphorylation of both PAK and cofilin in nArgBP2 KD (Fig. 3 *B* and *C*), indicating that nArgBP2 KD causes activation of WAVE1 and PAK, and a subsequent inactivation of cofilin. Furthermore, we found that the inhibition of PAK by the coexpression of PAK-inhibitory domain (PID) or the coexpression of a constitutively active cofilin mutant S3A (Fig. 3 *D–H*) both partially rescued the dendritic spine phenotype caused by nArgBP2 KD.

Because nArgBP2 KD activates both WAVE and PAK pathways, we reasoned that just inhibiting PAK may not be enough to rescue the phenotype fully. To prove this hypothesis, we decided to block both WAVE and PAK activity in nArgBP2 KD background. Previously, we found that among three SH3 domains of nArgBP2, the first and the second bind to WAVE, whereas the third does not (3). Thus, we constructed mitochondria-targeting SH3-1/2 and SH3-3 domains (mSH3-1/2 and mSH3-3). As expected, mSH3-1/2 (but not mSH3-3) sequesters WAVE from the cytosol to the mitochondria (Fig. S3). Using these tools, we showed that the sequestration of WAVE by mSH3-1/2 partially rescues the dendritic spine phenotype caused by nArgBP2 KD (Fig. S4). Furthermore, we demonstrated that the inhibition of PAK by PID or cofilin by S3A, combined with sequestration of WAVE by mSH3-1/2, almost totally rescues the aberrant spine phenotype caused by nArgBP2 KD (Fig. 3 *D–H*). Together, these results strongly indicate a causal relation between elevated WAVE/PAK/cofilin phosphorylation and the aberrant dendritic spine morphology observed in nArgBP2 KD neurons.

Previously we demonstrated that the ArgBP2/nArgBP2 KD in astrocytes causes major changes in actin dynamics (3). We have used live-cell imaging techniques to follow the spatial-temporal dynamics of actin in dendritic spines. We derived outline profiles of individual spines in successive time-lapse recording frames and used these profiles to calculate a shape factor (Fig. 4*A*, details are provided in *Materials and Methods*). Changes in shape factor during the time-lapse recording are an index of the spine motility. Consequently, we found that the shape factor value oscillates closer to 0.9 in control neurons (Fig. 4*B*), indicating that spines are stable and rounder in these cells. In nArgBP2 KD spines, however, wider fluctuations in the shape factor spanning from 0.4 to ∼0.8 were observed, suggesting the irregular shapes and the highly dynamic nature of KD spines (Fig. 4*C*).

To study the actin dynamics within spines further, we performed fluorescence recovery after photobleaching (FRAP) experiments in neurons expressing GFP-actin. Individual spines were photobleached, and the time of fluorescence recovery was used as an indicator of actin dynamics (Fig. 4*D*). Because actin filaments within the spines are in dynamic equilibrium, the recovery of fluorescence reflects the rate of turnover of actin.

In control spines, the average time constant for recovery of GFP-actin after photobleaching was 29.99 ± 1.65 s; 80.3 ± 1.14% of total actin was in a dynamic state, and 19.7 ± 1.09% was stable (Fig. 4 *E–G* and Table S1). In nArgBP2 KD, the rate of turnover of actin was not significantly altered ($\tau = 28.12 \pm 1.40$ s), but almost all actin (95.1 ± 1.16%) was in a dynamic state, whereas only 4.90 ± 0.54% of the total was stable (Fig. 4 *E–G* and Table S1). Finally, treatment of neurons with 10 μM N^6-[2-[[4-(diethylamino)-1-methylbutyl] amino]-6-methyl-4-pyrimidinyl]-2-methyl-4,6-quinolinediamine trihydrochloride (NSC23766), a selective inhibitor of Rac1-GEF, completely abrogated the effect of nArgBP2 KD on actin composition, indicating that Rac1 activation is downstream of nArgBP2 KD (Fig. 4 and Table S1).

Discussion

Here, we show that nArgBP2 ablation reduces the number of mushroom-shaped dendritic spines and selectively inhibits the spine-synapse formation. FRAP experiments revealed that nArgBP2 KD increases the pool of dynamic actin and diminishes the amount of stable F-actin. This alteration of actin dynamics correlates

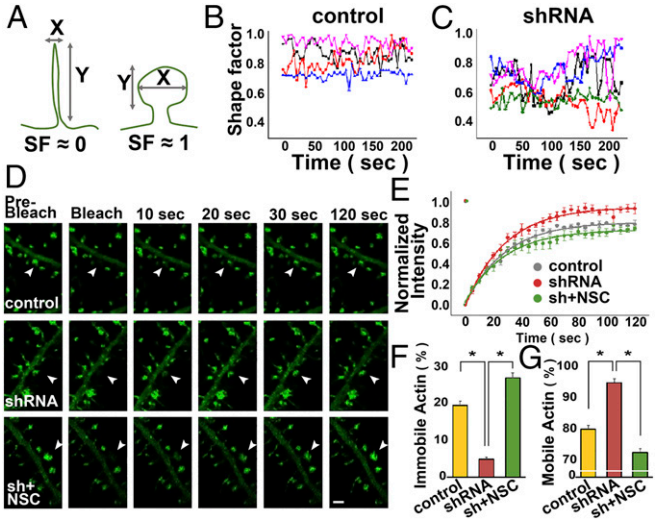

Fig. 4. nArgBP2 KD causes a marked increase of actin cytoskeleton dynamics in spines. (*A*) Shape factor (SF) of dendritic spines calculated from time-lapse recordings of GFP-actin dynamics. Changes in spine shape were assessed using the "shape factor" routine (sf = $4\pi A/p^2$) of the MetaMorph program. Values close to 0 represent elongated or ruffled shapes, whereas values around 1 describe a perfect circle. Fluctuations in shape factor values reflect spine motility. Representative shape factor profiles of control (*B*) and nArgBP2 KD (*C*) spines over time. Each color indicates an individual spine. Hippocampal neurons were transfected at DIV9 and analyzed at DIV16. Compared with control, nArgBP2 KD produces an irregular or elongated spine shape and a wider fluctuation of the shape factor that indicates rapid spine motility. (*D*) Example of fluorescence recovery in spines after photobleaching. Neurons were transfected with GFP-actin at DIV9 and studied at DIV16. Immediately after photobleaching, the images indicate a complete loss of fluorescence in the bleached spines (arrowheads), although neighboring spines are unaltered. Subsequent time-lapse images show gradual recovery of fluorescence. (Scale bar: 2 μm.) (*E*) Fluorescence intensity in the bleached spines, normalized to resting values. The continuous lines were given by Eq. S1. Fluorescence recovery was up to ∼80% and ∼98% in control neurons and nArgBP2 KD cells, respectively. Treatment of neurons with 10 μM Rac1 inhibitor NSC23766 completely abrogates the effect of nArgBP2 KD on actin dynamics. Proportions of immobile actin (*F*) and mobile actin (*G*) in control, nArgBP2 KD, and nArgBP2 KD spines treated with NSC23766 are shown (exact numbers are shown in Table S1). Results clearly show that nArgBP2 KD causes a dramatic increase in the fraction of dynamic actin and a concomitant reduction in the fraction of stable actin in spines. $^*P < 0.05$ by ANOVA, followed by Tukey's HSD post hoc test ($n = 15$ neurons from five independent cultures).

with the amplification of the shape factor fluctuation and the increase in the dendritic spine motility.

nArgBP2 knockout mice show manic/bipolar-like behavior resembling many aspects of BD (22, 23). The prefrontal cortex, striatum, and amygdala have been implicated in the pathogenesis of the disease (21, 36), all of which are brain regions that express nArgBP2 highly (20). Furthermore, a significant reduction in the average number of spines was found in individuals with BD (37). Therefore, the reduction of the mushroom-shaped spines and inhibition of the spine-synapse formation observed in this study are consistent with the spine phenotypes in individuals with BD.

The C-terminal SH3 domains of nArgBP2 bind to WAVE1 and WAVE2, and to components of a WAVE regulatory complex such as PIR121 and Nap1 (3). WAVE is controlled by Rac1 with the WAVE regulatory complex. We showed that nArgBP2 KD increases levels of the active pool of WAVE1 (Fig. 3*A*). These results are consistent with the increase in the dynamic pool of F-actin observed in nArgBP2 KD spines and support our previous observations that ArgBP2/nArgBP2 KD in astrocytes increases actin dynamics (3). Coherently with a global role of nArgBP2 in the repression of WAVE, we also observed a molecular signature of Rac1 activation in nArgBP2 KD. We found that both PAK and cofilin phosphorylation are elevated in nArgBP2 KD (Fig. 3 *B* and *C*). Accordingly, either the inhibition of PAK1 or the activation of cofilin combined with sequestration of WAVE compensates for the ablation of nArgBP2 and rescues spine defects (Fig. 3 *D–H*). In addition, the inhibition of Rac1 by NSC23766 successfully rescues the nArgBP2 KD phenotype in actin composition (Fig. 4 *E–G*). Thus, we propose that the recovery of spine formation through the inhibition of the Rac1/PAK1 pathway is due to the ability of cofilin to balance the burst of local polymerization of F-actin within spines caused by the overactivation of the WAVE pathway.

A recent study (27) demonstrated the physical interaction of nArgBP2 with Shank3, the loss of which is associated with autism spectrum disorders. Interestingly, transgenic mice overexpressing Shank3 show a hyperkinetic neuropsychiatric-like disorder, and higher levels of Shank3 increase local accumulation of F-actin in the dendritic spine through its direct effect on the Arp2/3 complex (25). Thus, nArgBP2, through its action on WAVE, which is closely interconnected with Shank3, regulates local polymerization of F-actin in spine glutamatergic synapses and may play a role in several neuropsychiatric disorders. Furthermore, PIR121, which interacts with nArgBP2 (3), is also called cytoplasmic fragile X mental retardation protein (FMRP) interacting protein 2 (CYFIP2) (38, 39), and FMRP-null neurons show a reduction in mushroom-shaped spines and a increase of filopodia-like structures (40), very similar to what we show here in nArgBP2 KD.

Finally, we observed a very striking absence of mushroom-shaped spines in nArgBP2 KD excitatory neurons and a preferential assemblage of synaptic contacts on the dendritic shafts. The shaft synapses are relatively high in young animals, but drop considerably during maturation. In an adult animal, however, spine synapses increase shortly after long-term potentiation (LTP) induction, and are converted into shaft synapses during LTP maintenance (41). Behavioral experience also alters spine and shaft synapses differently (42, 43). Epileptiform activity leads to loss of spine synapses, but not shaft synapses, whereas activity blockade induces a loss of shaft synapses (44). Therefore, the balance between spine-synapse and shaft-synapse controls neuronal efficacy, and any alteration of this equilibrium could lead to various psychiatric disorders. Indeed, a recent study showed that deletion of the autism-associated gene neurobeachin reduces the number of spinous synapses and forces excitatory synapses to terminate at dendritic shafts (45). Another related study showed that EphrinB3, whose signaling is also linked to anxiety disorders, autism, and mental retardation, selectively promotes synapse formation on dendritic shafts (46). Changes in the proportion of excitatory synaptic contacts formed either on dendritic spines or shafts should have significant effects on network function and plasticity (46–48). Previous studies, however, failed to produce generally accepted evidence on the net effect of an unbalanced ratio of these two types of synapse (46, 49–52). Our data demonstrate that the increase of synapses on dendritic shaft caused by nArgBP2 KD does not compensate for the alteration of excitatory synaptic transmission due to the loss of synapses on dendritic spines. Because the excitatory/inhibitory synaptic imbalance likely leads to a broad spectrum of neuropsychiatric disorders, the nArgBP2 KD that selectively alters excitatory synapse formation may account for manic/bipolar-like behaviors observed in nArgBP2 knockout mice. Moreover, because nArgBP2 interacts with proteins involved in different neurological disorders, such as autism, fragile X syndrome, and BD, our finding on the role of nArgBP2 in the regulation of excitatory synapse formation implies that it could function as a hub linking together etiological factors of different disorders. It

certainly helps to broaden the knowledge base around these diseases and will eventually contribute to identify novel molecular targets for their treatment.

Materials and Methods

Animal experimental procedures were approved by the Institutional Animal Care and Use Committee of Seoul National University (approval ID no. SNU-100930-5). Rat nArgBP2 cDNA was constructed as previously described (3). nArgBP2 KD was carried out by expressing shRNA duplexes through a pSIREN-DNR-DsRed vector. Primary rat hippocampal or cortical neurons derived from E18 Sprague–Dawley fetal rats were prepared as described previously (53). Images were analyzed using MetaMorph software and ImageJ. More information about the experimental procedures is available in *SI Materials and Methods*.

Note Added in Proof. While our manuscript was under revision, a study on the genetic ablation of Sorbs2 (nArgBP2) in mice was published that showed the reduction of dendritic complexity and excitatory synaptic transmission (22). Unlike our data, Sorbs2 knockout mice did not show significant alterations in dendritic spines. These observations were, however, conducted on dentate gyrus granule cells, which are constantly replaced by neurogenesis. Thus, further analysis of other brain regions would be necessary to better understand the effect of nArgBP2 ablation.

ACKNOWLEDGMENTS. This research was supported by Grant NRF-2015M3C7A1028790 from the Brain Research Program through the National Research Foundation of Korea and Grant 20100029395 from the Biomembrane Plasticity Research Center (to S.C.) funded by the Ministry of Science, ICT & Future Planning, Republic of Korea.

1. Kawabe H, et al. (1999) nArgBP2, a novel neural member of ponsin/ArgBP2/vinexin family that interacts with synapse-associated protein 90/postsynaptic density-95-associated protein (SAPAP). *J Biol Chem* 274(43):30914–30918.
2. Kioka N, Ueda K, Amachi T (2002) Vinexin, CAP/ponsin, ArgBP2: A novel adaptor protein family regulating cytoskeletal organization and signal transduction. *Cell Struct Funct* 27(1):1–7.
3. Cestra G, Toomre D, Chang S, De Camilli P (2005) The Abl/Arg substrate ArgBP2/nArgBP2 coordinates the function of multiple regulatory mechanisms converging on the actin cytoskeleton. *Proc Natl Acad Sci USA* 102(5):1731–1736.
4. Soubeyran P, Barac A, Szymkiewicz I, Dikic I (2003) Cbl-ArgBP2 complex mediates ubiquitination and degradation of c-Abl. *Biochem J* 370(Pt 1):29–34.
5. Wang B, Golemis EA, Kruh GD (1997) ArgBP2, a multiple Src homology 3 domain-containing, Arg/Abl-interacting protein, is phosphorylated in v-Abl-transformed cells and localized in stress fibers and cardiocyte Z-disks. *J Biol Chem* 272(28):17542–17550.
6. Haglund K, Ivankovic-Dikic I, Shimokawa N, Kruh GD, Dikic I (2004) Recruitment of Pyk2 and Cbl to lipid rafts mediates signals important for actin reorganization in growing neurites. *J Cell Sci* 117(Pt 12):2557–2568.
7. Stradal TE, et al. (2004) Regulation of actin dynamics by WASP and WAVE family proteins. *Trends Cell Biol* 14(6):303–311.
8. Kim Y, et al. (2006) Phosphorylation of WAVE1 regulates actin polymerization and dendritic spine morphology. *Nature* 442(7104):814–817.
9. Threadgill R, Bobb K, Ghosh A (1997) Regulation of dendritic growth and remodeling by Rho, Rac, and Cdc42. *Neuron* 19(3):625–634.
10. Ridley AJ (2006) Rho GTPases and actin dynamics in membrane protrusions and vesicle trafficking. *Trends Cell Biol* 16(10):522–529.
11. Sells MA, Chernoff J (1997) Emerging from the Pak: The p21-activated protein kinase family. *Trends Cell Biol* 7(4):162–167.
12. Arber S, et al. (1998) Regulation of actin dynamics through phosphorylation of cofilin by LIM-kinase. *Nature* 393(6687):805–809.
13. Bamburg JR (1999) Proteins of the ADF/cofilin family: Essential regulators of actin dynamics. *Annu Rev Cell Dev Biol* 15:185–230.
14. dos Remedios CG, et al. (2003) Actin binding proteins: Regulation of cytoskeletal microfilaments. *Physiol Rev* 83(2):433–473.
15. Hayashi ML, et al. (2004) Altered cortical synaptic morphology and impaired memory consolidation in forebrain- specific dominant-negative PAK transgenic mice. *Neuron* 42(5):773–787.
16. Golden SA, et al. (2013) Epigenetic regulation of RAC1 induces synaptic remodeling in stress disorders and depression. *Nat Med* 19(3):337–344.
17. Ramakers GJ (2002) Rho proteins, mental retardation and the cellular basis of cognition. *Trends Neurosci* 25(4):191–199.
18. Gilman SR, et al. (2011) Rare de novo variants associated with autism implicate a large functional network of genes involved in formation and function of synapses. *Neuron* 70(5):898–907.
19. Fromer M, et al. (2014) De novo mutations in schizophrenia implicate synaptic networks. *Nature* 506(7487):179–184.
20. Lein ES, et al. (2007) Genome-wide atlas of gene expression in the adult mouse brain. *Nature* 445(7124):168–176.
21. Strakowski SM, Delbello MP, Adler CM (2005) The functional neuroanatomy of bipolar disorder: A review of neuroimaging findings. *Mol Psychiatry* 10(1):105–116.
22. Zhang Q, et al. (2016) Impaired dendritic development and memory in Sorbs2 knockout mice. *J Neurosci* 36(7):2247–2260.
23. Feng G (2010) US Patent 20100077493 A1.
24. Welch JM, et al. (2007) Cortico-striatal synaptic defects and OCD-like behaviours in Sapap3-mutant mice. *Nature* 448(7156):894–900.
25. Han K, et al. (2013) SHANK3 overexpression causes manic-like behaviour with unique pharmacogenetic properties. *Nature* 503(7474):72–77.
26. Gauthier J, et al. (2009) Novel de novo SHANK3 mutation in autistic patients. *Am J Med Genet B Neuropsychiatr Genet* 150B(3):421–424.
27. Peça J, et al. (2011) Shank3 mutant mice display autistic-like behaviours and striatal dysfunction. *Nature* 472(7344):437–442.
28. Lin WH, Webb DJ (2009) Actin and Actin-Binding Proteins: Masters of Dendritic Spine Formation, Morphology, and Function. *Open Neurosci J* 3:54–66.
29. Hotulainen P, Hoogenraad CC (2010) Actin in dendritic spines: Connecting dynamics to function. *J Cell Biol* 189(4):619–629.
30. Zhang W, Benson DL (2001) Stages of synapse development defined by dependence on F-actin. *J Neurosci* 21(14):5169–5181.
31. Cingolani LA, Goda Y (2008) Actin in action: The interplay between the actin cytoskeleton and synaptic efficacy. *Nat Rev Neurosci* 9(5):344–356.
32. Yang N, et al. (1998) Cofilin phosphorylation by LIM-kinase 1 and its role in Rac-mediated actin reorganization. *Nature* 393(6687):809–812.
33. Boda B, Nikonenko I, Alberi S, Muller D (2006) Central nervous system functions of PAK protein family: From spine morphogenesis to mental retardation. *Mol Neurobiol* 34(1):67–80.
34. Nikolić M (2008) The Pak1 kinase: An important regulator of neuronal morphology and function in the developing forebrain. *Mol Neurobiol* 37(2-3):187–202.
35. Penzes P, et al. (2003) Rapid induction of dendritic spine morphogenesis by trans-synaptic ephrinB-EphB receptor activation of the Rho-GEF kalirin. *Neuron* 37(2):263–274.
36. Hajek T, Carrey N, Alda M (2005) Neuroanatomical abnormalities as risk factors for bipolar disorder. *Bipolar Disord* 7(5):393–403.
37. Konopaske GT, Lange N, Coyle JT, Benes FM (2014) Prefrontal cortical dendritic spine pathology in schizophrenia and bipolar disorder. *JAMA Psychiatry* 71(12):1323–1331.
38. Schenck A, et al. (2003) CYFIP/Sra-1 controls neuronal connectivity in Drosophila and links the Rac1 GTPase pathway to the fragile X protein. *Neuron* 38(6):887–898.
39. Schenck A, Bardoni B, Moro A, Bagni C, Mandel JL (2001) A highly conserved protein family interacting with the fragile X mental retardation protein (FMRP) and displaying selective interactions with FMRP-related proteins FXR1P and FXR2P. *Proc Natl Acad Sci USA* 98(15):8844–8849.
40. Comery TA, et al. (1997) Abnormal dendritic spines in fragile X knockout mice: maturation and pruning deficits. *Proc Natl Acad Sci USA* 94(10):5401–5404.
41. Geinisman Y, Detoledo-Morrell L, Morrell F, Persina IS, Beatty MA (1996) Synapse restructuring associated with the maintenance phase of hippocampal long-term potentiation. *J Comp Neurol* 368(3):413–423.
42. Helmeke C, Ovtscharoff W, Jr, Poeggel G, Braun K (2001) Juvenile emotional experience alters synaptic inputs on pyramidal neurons in the anterior cingulate cortex. *Cereb Cortex* 11(8):717–727.
43. Nikolakopoulou AM, Davies HA, Stewart MG (2006) Passive avoidance training decreases synapse density in the hippocampus of the domestic chick. *Eur J Neurosci* 23(4):1054–1062.
44. Zha XM, Green SH, Dailey ME (2005) Regulation of hippocampal synapse remodeling by epileptiform activity. *Mol Cell Neurosci* 29(4):494–506.
45. Niesmann K, et al. (2011) Dendritic spine formation and synaptic function require neurobeachin. *Nat Commun* 2:557.
46. Aoto J, et al. (2007) Postsynaptic ephrinB3 promotes shaft glutamatergic synapse formation. *J Neurosci* 27(28):7508–7519.
47. Sheng M, Hoogenraad CC (2007) The postsynaptic architecture of excitatory synapses: A more quantitative view. *Annu Rev Biochem* 76:823–847.
48. Yuste R (2011) Dendritic spines and distributed circuits. *Neuron* 71(5):772–781.
49. Mateos JM, et al. (2007) Synaptic modifications at the CA3-CA1 synapse after chronic AMPA receptor blockade in rat hippocampal slices. *J Physiol* 581(Pt 1):129–138.
50. Fu Z, et al. (2007) Differential roles of Rap1 and Rap2 small GTPases in neurite retraction and synapse elimination in hippocampal spiny neurons. *J Neurochem* 100(1):118–131.
51. Stamatakou E, Marzo A, Gibb A, Salinas PC (2013) Activity-dependent spine morphogenesis: a role for the actin-capping protein Eps8. *J Neurosci* 33(6):2661–2670.
52. Atkin G, et al. (2015) Loss of F-box only protein 2 (Fbxo2) disrupts levels and localization of select NMDA receptor subunits, and promotes aberrant synaptic connectivity. *J Neurosci* 35(15):6165–6178.
53. Zhao H, et al. (2014) SCAMP5 plays a critical role in synaptic vesicle endocytosis during high neuronal activity. *J Neurosci* 34(30):10085–10095.
54. Fischer M, Kaech S, Wagner U, Brinkhaus H, Matus A (2000) Glutamate receptors regulate actin-based plasticity in dendritic spines. *Nat Neurosci* 3(9):887–894.
55. Dunn KW, Kamocka MM, McDonald JH (2011) A practical guide to evaluating colocalization in biological microscopy. *Am J Physiol Cell Physiol* 300(4):C723–C742.